Revision 2

Pink colour in Type I diamonds: Is deformation twinning the cause?

Daniel Howell[1*], David Fisher[2], Sandra Piazolo[1],
William L. Griffin[1], Samantha J. Sibley[2]

[1] ARC Center of Excellence for Core to Crust Fluid Systems (CCFS) and GEMOC, Department of Earth & Planetary Science, Macquarie University, NSW 2109, Australia

[2] De Beers Technologies UK, De Beers Research Centre, Belmont Road, Maidenhead, SL6 6JW, UK.

* corresponding author: (T) +61(0)298504401, (F) +61(0)298508943, (e) daniel.howell@mq.edu.au

Abstract

Plastic deformation of diamond has long been associated with the generation of colour, specifically brown and pink. Extensive previous optical and spectroscopic characterization of natural pink Type I (nitrogen containing) diamonds has revealed two clear groupings, with distinct geographical origins. Group 1 pinks, which have low concentrations of nitrogen and are relatively highly aggregated (IaA≤B), have only been found in the Argyle lamproite pipe (Australia) and Santa Elena alluvial deposits (Venezuela). Group 2 pinks, which have much higher nitrogen concentrations and exhibit low levels of aggregation, have been found in deposits from southern Africa, Canada and Russia. Pink colour is intimately associated with deformation lamellae on the {111} crystal planes, and understanding their formation and structure has been a priority with respect to defining the source of this gemologically valuable colour center. In group 2 pinks, these {111} lamellae have been characterized as deformation microtwins by both transmission electron microscopy and X-ray diffraction. Subsequently the {111} lamellae in group 1 pinks have been assumed to also be deformation microtwins. In this paper we report electron backscatter diffraction (EBSD) studies of three brown and six pink naturally deformed diamonds with varying nitrogen concentrations and aggregation states. The results show that there are no deformation microtwins in the group 1 pink or brown diamonds. The study also highlights the usefulness of orientation contrast imaging as

a simple and rapid method for determining the presence of microtwins. Our results suggest that the colour in the group 1 pink diamonds is not directly related to the presence of deformation twins. However, we propose that twins may have been present but subsequently removed by de-twinning, a process that utilizes the same Shockley partial dislocations involved in the original twinning event. Therefore it maybe the process of twinning (and de-twinning) that creates the defect responsible for pink colour, as opposed to the actual structure of microtwins themselves. In addition, a large laboratory dataset of pink diamond analyses reveals the occurrence of group 1 pink diamonds in the Namibian marine (secondary) deposits. This would appear to suggest an additional source of group 1 pink diamonds in southern Africa, but the antiquity of these diamonds means that a common source on the former Pangaea supercontinent cannot be ruled out.

Keywords: Shockley partial dislocations, plastic deformation, de-twinning, Argyle, electron backscatter diffraction (EBSD), nitrogen aggregation

Introduction

It has long been recognized that brown and pink colours in diamonds are associated with plastic deformation (Collins, 1982). The colour is often confined within {111} lamellae while the bulk of the crystal is colourless (Collins et al., 2000), a phenomenon commonly referred to by gemologists as “graining”. Like other face-centered cubic (FCC) materials, diamond exhibits a {111}<110> slip system, meaning that the {111} planes are the active slip planes with movement in the <110> direction. Due to the high symmetry of diamond, the {111} planes are also twin planes. Twins in diamond are contact twins, where reflection in a {111} plane is the equivalent of a 60° rotation around a <111> axis (**Figure 1**). Note that in a twin, lattice points in one crystal are shared as lattice points in another crystal, adding apparent symmetry to the crystal pairs; hence twinning adds symmetry to the crystal, decreasing the energy stored within it. They commonly occur as arrays of twins parallel to one another (i.e. polysynthetic twins). Twinning in diamond can occur during growth (e.g. Yacoot et al., 1998; Machado et al., 1998; Tomlinson et al., 2011) or during deformation (Buerger, 1945; Hirth & Lothe, 1982; Christian & Mahajan, 1995; Niewczas, 2007). Early work using indentation (Phaal, 1964) and high-pressure

high-temperature (HPHT) experiments (de Vries, 1975) produced deformation microtwins, which were also observed in natural samples (Varma, 1970). More recent studies using transmission electron microscopy (TEM; Shiyaev et al. 2007; Gaillou et al., 2010), X-ray diffraction (Titkov et al., 2012), electron backscatter diffraction (EBSD, Howell et al., 2012a) and atomic force microscopy (AFM; Gainutdinov et al., 2013), have shown these analytical techniques to be powerful tools for identifying some of these {111} lamellae as deformation microtwins.

Much of the recent research into plastic deformation of natural diamonds has focused on its influence on colour, due to its gemological value. Pink diamonds are exceptionally rare; by our calculations they make up less than 0.0001% (by carat weight) of the annual total global diamond production. This calculation is based on Arygle's 2013 production of 10 million carats, <0.1% of which are stated as being pink, which represents an estimated 90% of global pink diamonds, and a total global diamond production of 155 carats for 2013. While both brown and pink diamonds exhibit characteristics of plastic deformation, colourless diamonds can also exhibit these same features. Annealing at HPHT conditions can remove the colour of brown diamonds (Fisher, 2009); in certain Type IIa diamonds (nominally nitrogen-free, as determined by Fourier Transform infrared (FTIR) absorption spectroscopy) such heat treatment may reveal an underlying pink colour (Hounsome et al., 2006; Fisher et al., 2009). While the cause of brown colour has recently been shown to be the result of vacancy clusters generated by plastic deformation (Fisher, 2009), the specific defect responsible for the relevant absorption that creates pink colour is yet to be identified. The pink {111} lamellae were proposed by Mineeva et al. (2007; 2009) to be deformation microtwins; this was subsequently confirmed by transmission electron microscopy (TEM; Gaillou et al., 2010) and X-ray diffraction (Titkov et al., 2012) analysis of natural pink diamonds. HPHT experiments have also generated microtwins while deforming diamonds (Shiryaev et al., 2007; Howell et al., 2012a), but not the pink colour. These findings have generated increased interest in understanding the possible role that these crystallographic features play in the formation of pink colour.

Recently, extensive categorization of Type I (i.e. nitrogen containing) gem-quality pink diamonds by Gaillou et al. (2010; 2012) identified two distinct groups. The

primary crystallographic and spectroscopic features of these two groups of diamonds are listed in **Table 1.** The key differences between them are:

(1) Spatial distribution of colour. In both groups of pink diamonds, the colour is closely associated with the {111} lamellae. In group 1 pinks, the lamellae appear predominantly wavy, and their number and width vary between samples. In contrast, in group 2 diamonds the lamellae are straight, with thicknesses ranging from 0.5 – 1 μm. While their distribution throughout the crystal can vary widely between samples, it is not uncommon for two or three lamellae to be close to each other, with the bulk of the crystal being colourless. Consequently, group 1 diamonds can *generally* have larger pink-coloured volumes than group 2.

(2) Distinction of {111} lamellae. In group 1 pinks, the {111} lamellae are far less distinct than in group 2 pinks when observed between crossed polarizers and by cathodoluminescence (CL) imaging. Birefringence patterns of group 1 diamonds are parallel to the {111} lamellae and therefore to the pink graining, but they can also show deformation on an additional set of {111} planes that does not correspond to any colour zonation. Birefringence reveals that the residual strain in the diamond is held within both pink and colourless volumes. The CL response of group 1 pinks has a grainy, irregular pattern, and the {111} lamellae are not always obvious. Group 2 pinks exhibit far more discrete {111} lamellae. While the birefringence patterns are again parallel to the lamellae, they reveal that the residual strain is much more focused about the lamellae and not distributed throughout the bulk of the crystal. The CL response of group 2 pinks shows their growth stratigraphy in the same way as non-deformed Type I diamonds, but the lamellae clearly cut across the growth banding. However, the emission intensity is not necessarily homogeneous along an individual lamella. The specific spectroscopic defects observed in both groups of pink diamonds are listed in **Table 1**.

(3) Nitrogen characteristics. Group 1 pink diamonds have relatively low nitrogen concentrations, and the N is commonly quite highly aggregated (> 50% IaB). Conversely, group 2 pinks have relatively higher nitrogen concentrations but lower aggregation states (<50% IaB).

(4) Geographical occurrence. Group 1 pink diamonds have only been reported from the Argyle lamproite pipe (Australia) and the Santa Elena alluvial deposits (Guaniamo area, Venezuela), while group 2 pinks have been found in a much larger range of localities, including southern Africa, Russia and Canada. No single deposit has been reported to contain both groups of pink diamonds.

It is important to note that the analytical confirmation that the {111} lamellae are microtwins has only been achieved for group 2 pink diamonds. It is often assumed that microtwins are also present in group 1 pinks, but this has not yet been proven. In this study we have aimed to confirm the presence or absence of these microtwins in the different categories of plastically deformed diamonds, as well as to determine the role that deformation twinning may play in creating defects responsible for colour. To do this we report FTIR and EBSD data from a collection of naturally deformed Type I diamonds of both pink and brown colour with varying nitrogen contents and aggregation states. We also provide a large, previously unpublished, FTIR dataset for pink diamonds from various geographical sources to supplement the existing data in the literature, and to test the groupings of Type I pinks by Gaillou et al. (2010; 2012).

Analytical Techniques

Fourier transform infrared spectroscopy (FTIR) was performed using a Nicolet Magna IR 750 FTIR spectrometer (De Beers Technologies UK) in direct microscopic mode. All spectra were fitted to standard absorption spectra for the A, B and D components using the CAXBD97.xls spreadsheet to obtain nitrogen concentrations and aggregation states (see Howell et al., (2012b) for further information on this method). Platelet characteristics (peak height, position and integrated area / intensity) are also reported, along with noting whether there is a hydrogen-related band at 3107 cm^{-1} present.

CL intensity images were collected on cleaned and carbon-coated samples on a Zeiss EVO 15 Scanning Electron Microscope (SEM; Geochemical Analysis Unit, Macquarie University). Accelerating voltages were varied between 15 and 25 kV to obtain the best quality images. The same SEM was used to obtain EBSD overview

maps of the bulk of each sample, using 20 kV accelerating voltage, 8 nA current and high vacuum. Higher-resolution EBSD analyses were performed using a field emission Zeiss Ultra Plus SEM (ACMM, Sydney University) to confirm the presence or absence of micro-twins, with acceleration voltages varied between 15-20 kV.

EBSD patterns obtained from both SEM instruments were automatically indexed using AZTEC software from HKL Technology – Oxford Instruments. For EBSD analysis, the specimen is itself tilted by 70° with respect to the incoming electron beam. Diffraction patterns were acquired on rectangular grids by moving the electron beam at a regular step size, ranging from 3 – 10 μm for the overview maps, and 0.05 – 0.2 μm for the high resolution maps, allowing for a detailed inspection of the {111} lamellae and surrounding crystal. All samples were investigated by both low- and high-resolution EBSD analysis. In addition to this, high-resolution orientation contrast (OC) images were taken, using a combination of two forescatter detectors (BSE detectors) that are positioned at a high angle to the specimen (Prior et al. 1996, 1999). If samples do not have a perfectly flat surface, the observed grey-scale variations in the OC images result from the combined effect of variations in crystallographic orientation and topography. Data processing protocols as detailed by Howell et al. (2012a) were followed. Representation of EBSD data includes colour-coded maps and crystal orientations depicted as three-dimensional cubes. Mean misorientation values are calculated by the AZTEC software for the overview maps, to provide a semi-quantitative measure of deformation at the sample scale.

Samples

Nine Type I natural diamonds (three browns and six pinks) were analysed in this study (**Figure 2**), all provided by De Beers Technologies UK. Source information for these samples is provided in **Table 2** where known. All of the samples have at least 2 parallel polished faces, while many are cut and polished on several sides creating cubes or other polyhedral forms. As shown by the orientation data provided in **Figure 2**, many of the samples have a set of polished {110} faces that are perpendicular to the {111} planes on which the deformation lamellae occur. This has been done to guarantee that the lamellae intersect a polished face and can therefore be analysed.

Results

Colour and Cathodoluminescence

All three brown diamonds show very heterogeneous colour distribution. Samples A6-03 and A6-05 exhibit obvious colour graining that correlates with features observed in the CL. The distribution of colour in A301-MB22 also appears to correlate with the CL but the graining is less distinct in this sample due to the crystal orientation, i.e. the polished faces are cut at a lower angle to the <111> direction (**Figure 2**). It is interesting that in both A6-03 and A6-05, the CL images show signs of slip having occurred on two sets of {111} planes (NE-SW and NW-SE, **Figure 2**), but the colour graining only occurs on one of the sets (NE-SW). Only A6-05 reveals obvious signs of growth stratigraphy in the CL, but this may simply be a result of the orientation in which the sample has been prepared.

Of the six pink samples, three have poorly defined colour graining (A62-06, A167-P1, and A62-12; **Figure 2**) when compared to the other three samples (NL000-PK11, NL000-PK46-A and NL000-PK01; **Figure 2**), in which it is very well defined. In samples A62-06, A167-P1, and A62-12 the graining correlates only weakly with the features observed in CL, which are very grainy or patchy in all three samples. Growth stratigraphy is present but not as cleanly defined as is commonly seen in other Type I diamonds. Some broad deformation features can be seen running vertically in A62-06, while in A167-P1 they run at an angle from top left to bottom right (both orientations are {111} planes; **Figure 2**). While these do correlate with the orientation of the pink graining, they do not have the same distinct appearance as the lamellae observed in the brown diamonds. In sample A62-12 we cannot see any CL features that may correlate with the two possible graining directions observed under normal light.

In samples NL000-PK11, NL000-PK46-A and NL000-PK01, most of the sample volume is colourless, and the pink colour is restricted exclusively to distinct planes orientated parallel to one or multiple {111} planes. In NL000-PK01, the graining looks much broader and the colour is more dispersed throughout the sample, but this is simply a result of the sample surface being cut at a lower angle to the <111>

direction (**Figure 2**). The CL response of all three samples shows well-defined growth stratigraphy, while the colour graining correlates with clearly observable {111} planes that cut across the growth stratigraphy (zoomed in images in Figure 2). These lamellae are less than 1 μm wide and the spacing between them varies from 15 to 500 μm.

FTIR Data

Figure 3a shows a plot of nitrogen aggregation state as a function of total nitrogen concentration for the nine diamond samples analysed in this study (**Table 2**). The three brown diamonds have quite high nitrogen concentrations (409 – 564 ppm) with varied aggregation states (8 – 52 % IaB). The six pink diamonds appear to split into two distinct groups. Samples A62-06, A167-P1, and A62-12, have low nitrogen concentrations (31 – 62 ppm) and are highly aggregated (71 – 77 %IaB) considering the low concentration. The other three pink samples, NL000-PK11, NL000-PK46-A and NL000-PK01 have nitrogen concentrations similar to the three brown samples (443 – 601 ppm) but consistently low aggregation states (2 – 16 %IaB). All nine diamonds exhibit a band at 3107 cm^{-1} related to the presence of hydrogen and show some evidence of platelets (1361 – 1376 cm^{-1}; **Table 2**), albeit very small B´ bands in the case of the three low-nitrogen concentration pinks (**Figure 3b**).

Figure 3c shows the same plot of nitrogen aggregation *vs* total nitrogen concentration as in **Figure 3a** but with an additional large dataset of pink diamonds from a range of localities (**supplementary data**). It can be clearly seen that the pink diamonds separate out into two different categories. The first shows relatively high aggregation state for a given total nitrogen concentration, generally below about 200 ppm. The second exhibits a wide range of nitrogen concentrations from about 150 ppm to 1600 ppm, but all show relatively low aggregation, typically below about 35%. The higher-aggregation population is dominated by stones from Argyle, with a few examples from Namibia's combined onshore alluvial deposits and offshore dredging operations. The characteristics of these stones are consistent with those already defined as group 1 pink diamonds by Gaillou et al. (2010; 2012). The lower-aggregation category contains diamonds from a number of localities including South African productions

(Finsch and De Beers Pool are kimberlite deposits; Koingnass and Tweepad are alluvial), Canada's Victor mine (kimberlite) and other stones from the Namibian productions. Pink diamonds from the Siberian Internatsional'naya kimberlite (Titkov et al., 2008) also fall into this category, exhibiting low aggregation and significant nitrogen concentrations, and classify as group 2 pinks.

EBSD Data

All of the nine analysed samples show minor crystal orientation changes, with mean misorientation values (calculated from the overview maps and therefore representing changes across the whole sample) on the order of 0.5 – 1.1^{o} (Table 3). None of the samples shows any distinct patterns in their crystal lattice distortion at the resolution of the overview EBSD maps (3 – 10 μm; examples given in **Figure 4**), nor do they show any obvious relationship to the deformation lamellae observed under CL. At this coarse scale, it is not possible to determine if any of the {111} lamellae are microtwins by EBSD. However, the lamellae are observed in the OC images of the some of the pink diamonds and they correlate to those seen under CL (**Figure 5**).

By looking at the samples in greater detail with the high-resolution EBSD analysis, distinct differences can be observed. The three brown diamonds show mean crystal misorientations (derived from the overview EBSD maps) between 0.75 – 0.96^{o} (**Table 3; Figure 4a**). The {111} deformation lamellae visible in CL were not observed in the OC images or the high-resolution EBSD patterns (data not shown), suggesting they are not microtwins.

Treating the pink diamonds as two populations (as defined by their pink colour distribution [**Figure 2**] and nitrogen characteristics [**Figure 3, Table 2**]) allows some interesting comparisons. The changes in mean crystal misorientation derived from the overview EBSD maps of A62-06, A167-P1, and A62-12 (i.e. the three pink samples with low N concentrations and high aggregation states), ranges from 0.49 – 1.11^{o} (**Table 3; Figure 4b**). The {111} lamellae are not observed in the OC images, and the high resolution EBSD analysis shows that no microtwins are present at the 50 nm scale (data not shown).

The three pink samples with higher nitrogen concentrations and low aggregation states (NL000-PK11, NL000-PK46-A and NL000-PK01; Table 2) show changes in mean crystal misorientation from 0.46 – 0.94^{o} (**Table 3**). Again, there appears to be no obvious relationship between the deformation recorded in the overview EBSD maps and {111} lamellae (**Figure 4c**). In contrast to the other 6 samples, the {111} lamellae observed in the CL of these three samples are clearly visible in the OC images (**Figure 5**). In most cases the lamellae stretch all the way across the crystal, but in a few cases they terminate within the body of the crystal (arrows in **Figure 5b and c**). In NL000-PK46-A, there is a single deformation lamella that is in a different <111> orientation to the others that crosscuts the main set of {111} lamellae (arrow in **Figure 2**). Where two lamellae intersect, there appears to be a cavity in the sample of unknown depth (**Figure 5f**). High-resolution EBSD analysis of the deformation lamellae in these three pink diamonds confirms them to be microtwins (**Figure 6**). Two twin planes define each lamella, with the enclosed domain representing a characteristic {111} twin relationship, with a 60^{o} rotation about one of the <111> directions of the parent lattice.

Discussion

The brown diamonds studied here reveal no evidence of containing microtwins. The {111} deformation lamellae that control the colour graining and are visible in the CL response are therefore interpreted to be slip planes. This finding is in agreement with those of Howell et al. (2012a) who found no microtwins in two brown diamonds from Finsch. There is also no discernable difference in the amount of crystal misorientation observed in these brown diamonds when compared with the six pinks.

Based on the FTIR data and the colour distribution in the six pink diamonds, it is clear that they can be separated into the two groups defined by Gaillou et al. (2010; 2012). Samples A62-06, A167-P1, and A62-12 have the characteristics of group 1 pink diamonds: low nitrogen concentrations with high aggregation states; less well-defined colour graining that correlates poorly with features observed in the grainy CL; two of them come from the Argyle mine. Samples NL000-PK11, NL000-PK46-A and NL000-PK01 are group 2 pink diamonds. They have above-average nitrogen

concentrations and low levels of aggregation; the pink colour is clearly related to {111} lamellae observed in CL and EBSD; the CL also shows the clear growth stratigraphy typical of Type I diamonds; the samples all come from either kimberlites (Finsch) or alluvial deposits (Koingnass and Tweepad) in South Africa.

One further difference between these two groups of diamonds is that deformation microtwins are present in group 2 pinks, but absent in the group 1 pinks. While previous studies had confirmed that the {111} lamellae in group 2 pinks were microtwins (Gaillou et al., 2010; Titkov et al., 2012), there was only an assumption that this was also true of group 1 pinks. The data presented in this study suggest that this is not the case. We acknowledge that EBSD is only a surface technique, so if the lamellae did not intersect and therefore outcrop on the studied crystal face, then they would not be analysed. However, there is no evidence from optical observations that the lamellae observed in samples A62-06, A167-P1, and A62-12 all terminate below the prepared surface. Another possible reason for not recording twins in these group 1 pinks could be that the lamellae are too thin to be detected. TEM analysis by Gaillou et al. (2010) revealed that a single {111} lamella (~1 μm wide) could contain multiple twin domains (up to 6; see their Figure 17) which were only ~20 nm wide. If such thin twin domains were distributed within the group 1 pink diamond samples of this study, then the high-resolution EBSD analysis would not detect them, as the activation volume for EBSD analysis on carbon is larger than 20 nm. However, with the resolution of the OC imaging it should still be possible to observed such features. It is important to note that the multiple-twin domain structure of a single lamella, as reported by Gaillou et al. (2010), was not seen in the group 2 samples studied here. In contrast, our EBSD data and OC images have revealed only a single twin domain in each lamella studied. With all this is in mind, we are confident in our conclusion that microtwins are not present in the group 1 pink diamonds studied here.

Relationship Between Deformation Twinning and Pink Colour

As deformation microtwins do at least occur in group 2 pink diamonds, it is important to understand how they form, to better determine what role they might play in generating defects (and therefore possible colour centres) in diamond. Slip and

369 twinning are two of the main deformation modes that allow a solid to change shape
370 under the action of an applied stress. The classic definition of twinning states that the
371 twin and parent lattices are related to each other by a reflection in some plane (see
372 Yacoot et al., 1998). In diamond this reflection or mirror plane is {111}. In principle,
373 deformation twins form by a homogeneous simple shear of the original crystal lattice,
374 implying highly-coordinated displacements of individual atoms (Christian &
375 Mahajan, 1995). In an FCC lattice, this is accomplished by a displacement of $\frac{a}{6}\langle 112\rangle$
376 applied successively to {111} layers on the twinning plane (Niewczas, 2007). In
377 practice, this occurs by passing Shockley partial dislocations with a $\frac{a}{6}\langle 112\rangle$ Burgess
378 vector over every {111} plane above the twin plane (Niewczas, 2007; Li et al., 2011).
379 Work by Li et al. (2011) on FCC materials suggests that the twinning dislocations (i.e.
380 Shockley partial dislocations) can be activated in a cooperative and synchronized
381 manner, resulting in an almost simultaneous passage through the lattice. This process
382 effectively and efficiently relieves the local stress concentration, gives the crystal an
383 additional symmetry, generates significant shear strains in the collectively slipped
384 layers, and is clearly not just random atomic shuffling.
385
386 There are three possible conclusions to the question of whether deformation
387 microtwins are responsible for, or related to pink colour in diamonds.
388
389 (1) Pink colour is unrelated to microtwins in both group 1 and group 2 pink diamonds,
390 and the spatial relationship of the colour to the microtwins is purely coincidental.
391
392 (2) Pink colour is related to microtwins in group 2 pink diamonds but not in group 1
393 pink diamonds, implying that there are two different defects that cause pink colour in
394 Type I diamonds, or alternatively two different mechanisms capable of creating the
395 same defect.
396
397 (3) Pink colour is related to microtwins in both group 1 and group 2 pink diamonds.
398
399 As deformation microtwins have been identified in some group 2 pink diamonds
400 (Gaillou et al., 2010; Titkov et al., 2012), this crystallographic feature is a serious

contender for being intrinsic to the generation of pink colour. The fact that the pink colour is so closely related spatially to the twin planes provides support to this argument, and therefore undermines conclusion (1) above. However, the EBSD data from this study have shown no evidence of microtwins being present in the group 1 pink diamonds analysed. This would appear to undermine conclusions (3), but before we rule it out completely, we should consider an alternative. Instead of saying that group 1 pink diamonds never contained microtwins, we can consider that they no longer contain microtwins. Could group 1 pinks have contained microtwins that were subsequently removed?

While there is no evidence that these twins would be unstable at high temperatures, and would not be annealed like some other defects (e.g. vacancy clusters), recent studies in FCC metals have shown that a secondary twinning event may result in de-twinning (Cao et al., 2013). This is achieved by interaction of more partial dislocations with the twinned region, undoing the effects of the original twinning process. However, experiments in calcite have shown that de-twinning is not exactly the reverse of the twinning process, and that the de-twinned region can contain dislocation clusters (Kaga and Gilman, 1969). De-twinning is proposed to be a common process in FCC materials with low stacking-fault energies (Cao et al., 2013). Diamond's stacking-fault energy is higher than that of many FCC metals (Pirouz et al., 1983; Persson, 1983), but is still relatively low compared to other minerals, allowing for the possibility that de-twinning could occur. In some materials, deformation twinning and de-twinning have been reported to occur concurrently and to compete with each other (Ni et al., 2011).

As de-twinning has never been reported in diamonds, and there is very little about it in the mineralogy literature, we simply speculate that it could occur. If the diamonds were subjected to extended or multiple deformation events, or deformation at higher temperatures, then there is definitely potential for the de-twinning process to have occurred. It might account for some of the differences between group 1 and group 2 pinks. Additional or a secondary set of partial dislocations interacting with existing microtwins, would alter the appearance of these domains, making them wavy and less well defined, and could potentially generate more defects causing pink colour. This would produce more intense colour that is not so clearly related to the original twin.

However, if this de-twinning process has occurred, we might expect to find examples in the group 1 pinks of twins that had not been completely de-twinned. These have not yet been observed, but the number of samples examined in sufficient detail is still very small, and the twins would have to appear on the analysed surface.

The difference between conclusions (2) and (3), comes down to whether or not group 1 pink diamonds originally contained microtwins. Conclusion (2) suggests that if group 1 pinks never contained microtwins, and the pink colour in group 2 pinks is related to the presence of microtwins, then either a different defect causes pink colour in group 1 pink diamonds, or there is a different mechanism capable of producing the same defect as found in group 2 pink diamonds. The alternative, and potentially simpler conclusion (3) is that pink colour is related to microtwins in both groups of pink diamonds (i.e. same defect and same mechanism producing it), and that the microtwins have been removed by de-twinning in the group 1 pink diamonds. If this were the case, it would imply that the pink colour defect is related to the twinning (and de-twinning) process and not directly with the structure of the microtwin itself.

This study cannot confirm one of the three conclusions as being correct, as it was not designed to determine the exact structure of the defect responsible for pink colour. The finding from the EBSD analysis that no microtwins occur in group 1 pink diamonds initially appeared to rule out conclusion (3), but the possibility that de-twinning may have occurred means this remains a viable mechanism. What this work has done is to direct future research into the cause of pink colour in diamond. It is important to understand which defects maybe generated by the Shockley partial dislocations that are required for the twinning process, and to confirm whether or not the de-twinning process could take place in diamonds.

Timing of Deformation and the Mantle Conditions

A common question considered by diamond researchers is, when did the deformation take place? Is it during the diamonds' residence in the mantle, or is it associated with transportation and emplacement into the crust by kimberlites and lamproites? To assess this requires knowledge of how quickly the colour-causing defect forms, as well as its stability at mantle conditions. These factors are known for brown

diamonds, allowing calculations to be performed that suggest brown diamonds could keep their colour for millions of years if stored at or below 1000°C, while higher temperatures towards the base of the subcontinental lithospheric mantle (SCLM) might reduce or eliminate brown colour within thousands of years (Smith et al, 2010). For pink diamonds this assessment is not possible, as the defect responsible remains unknown. All that is known is that deformation twinning can occur very quickly prior to any crystal bending taking place (Howell et al., 2012a).

Commonly, the nitrogen concentration and aggregation data are used to infer differences in the age of the diamond, or the average mantle temperature at which it has resided (see Howell et al. (2012c) and references therein, for detailed discussions about the nitrogen-aggregation process and limitations of the data interpretation). Group 1 pinks have low N concentrations that are highly aggregated. Initially ignoring the possible effects of deformation on the aggregation process, this would imply a very long mantle residence time (>3 Ga) at temperatures ~1200°C (**Figure 3a**), or a much shorter time at higher temperatures (~200 Ma at 1300°C). Conversely, group 2 pinks have higher nitrogen concentrations that exhibit much lower aggregation states. Again, ignoring the effects of deformation, this would suggest moderate mantle residence times (<1.5 Ga) at temperatures ~1100°C (**Figure 3a**), or very short residence times at higher temperatures (<30 Ma at 1200°C).

These calculations show that the time – temperature relationship of the nitrogen aggregation process is far more sensitive to temperature than to time. Small temperature changes significantly move an isotherm on a plot of N concentration *vs* aggregation, whereas changes of billions of years have less effect (see different isotherms on **Figure 3a**). As a result, while it is possible to interpret a significant age difference between two groups of pink diamonds (assuming the same average temperature), it can also be more easily attributed to a small difference in mantle residence temperatures. If group 1 pinks are much older and have resided in the mantle for billions of years, then this would increase the possibility of multiple deformation events occurring (possibly resulting in de-twinning). Alternatively, if they have resided at higher temperatures, then group 1 pinks may have been more prone to deformation and/or been able to deform via mechanisms not possible at lower temperatures. The platelet data also support these two possible scenarios. The

group 1 pinks are more consistently *irregular* (Woods, 1986; **Figure 3b**), suggesting they have experienced either more sustained / multiple deformation events or higher residence temperatures than the less consistently *irregular* group 2 pinks.

As the effects of deformation on the nitrogen aggregation process are not well understood (e.g. Shiryaev et al., 2007), it is difficult to assess the validity of the above conclusions. While some workers have suggested that the additional vacancies created during deformation would enhance the rate of aggregation (Collins, 1980), others have suggested that B centres could be broken down, therefore reducing the measured aggregation state (Byrne et al., 2012). Assuming a faster rate of nitrogen aggregation due to deformation means that both sets of diamonds are either younger than first assessed, or formed at lower temperatures. The alternative effect, a reduced aggregation state, means that they are either older than first assumed, or formed at higher temperatures. Either way, the above conclusion that there is either a significant age difference between two groups of pink diamonds (assuming the same average temperature), or a difference in average mantle residence temperatures, would appear valid (assuming the effects of plastic deformation on nitrogen aggregation are the same in both sets of diamonds).

Pink diamonds are very rare; if microtwins are only found in pink diamonds (and possibly only 10% of all pink diamonds), the physical environment necessary for their formation in the mantle (i.e. PT conditions, a source of deviatoric stress and a host material capable of transferring this to the diamond) must also be exceptionally rare. Our understanding of the conditions required for this twinning process to occur is extremely lacking. While de Vries (1975) determined the stability field for the transition from brittle to ductile behaviour of diamond at HPHT conditions, this was based on the appearance of {111} deformation lamellae, which may have been slip planes or microtwins. A more detailed experimental program investigating the PT field and the differential strain rates necessary to generate deformation microtwins is required to better understand the nature of the mantle. Further insights may also be gained by investigating the kimberlites / lamproites of the deposits containing pink diamonds, and in particular the xenoliths that contain the diamonds.

Geographic Sources of Group 1 Pink Diamonds

As mentioned above, there have been no reports of a single primary deposit containing both group 1 and 2 pink diamonds. The data presented in **Figure 3c** expand the occurrence of group 1 pinks to include not only the Argyle and Santa Elena deposits, but also to an unknown deposit in southern Africa, which contributed diamonds to the Namibian alluvial deposits. However, as both the Namibian and Santa Elena deposits are secondary, it is difficult to make any strong connections between them to better understand their formation. It is possible that these group 1 pink diamonds do come from the same primary source. Considering their great age, diamonds from a primary source within the Pangaea supercontinent could have been spread over a wide area that included the future African and South American continents.

However, Gaillou et al. (2012) did note a significant connection though that will probably form the basis of future investigations into the geographical source and conditions of formation for group 1 pink diamonds. A comprehensive study of more than 5000 diamond crystals and fragments from the Guaniamo area (which contains the Santa Elena alluvial deposit) by Kaminsky et al. (2000) noted three significant similarities with those from Argyle: (1) a high proportion of eclogitic inclusions (2) very high mean temperatures of diamond formation (based on P-T estimates from the inclusions), and (3) high levels of Ti and Na in garnet, and Ti and K in clinopyroxene inclusions in the diamonds. Both sets also show high levels of nitrogen aggregation (Taylor et al., 1990), although the range of nitrogen concentrations in the Venezuelan samples appears much larger. Kaminsky et al. (2000) also highlighted that both deposits are associated with magmas that intruded Proterozoic cratons (rather than the more typical Archean cratons) relatively soon (<1 Ga) after a major rifting and magmatism events. This means they could reflect a distinctly different tectonothermal history from the diamonds found in Archean cratons.

Implications

The results from this study have provided important insights in both the analytical and geological fields. From an analytical perspective, this study has shown the power of EBSD in identifying microtwins in diamond. More importantly, it has shown that

simple orientation-contrast images are sufficient to confirm whether {111} deformation lamellae are microtwins or not. The quantitative deformation data obtained from the EBSD analysis are useful to investigate larger-scale permanent strain patterns, complementing the *in situ* analysis of elastic strain by confocal Raman spectroscopy (e.g. hyperspectral mapping of the microtwins and surrounding parent crystal; Gaillou et al., 2010).

From a geological perspective, this study reports new nitrogen concentration and aggregation data that expand the occurrences of group 1 pink diamonds beyond just Argyle and Santa Elena (Gaillou et al., 2010; 2012) to include a secondary deposit in southern Africa, the primary source of which remains unidentified. It is possible that the Santa Elena and southern African group 1 pinks are from the same primary source.

From a mineralogical perspective, the EBSD data reported here have shown that previous assumptions that microtwins are present in group 1 pink diamonds appear to be unfounded. This would initially appear to rule out deformation twinning as an integral process in generating the defect responsible for pink absorption in group 1 pink diamonds. So the obvious conclusions are that either the strong spatial relationship between pink colour in group 2 pink diamonds and microtwins are coincidental and that microtwins have no involvement with the pink defect, or that microtwinning is involved in creating colour only in group 2 pink diamonds. This would mean that a different defect is responsible for causing colour in group 1 pink diamonds, or that the same defect can be generated by multiple mechanisms. However, if the poorly understood process of de-twinning has occurred in group 1 pink diamonds, the conclusion that pink colour is generated by deformation microtwinning in both group 1 and 2 pink diamonds cannot be ruled out. While we see no evidence of microtwins in group 1 pink diamonds now, they may once have existed and been subsequently removed. Therefore we cannot confirm or rule out the role that deformation microtwinning may play in the formation of colour-causing defects. Future research into the specific defect responsible for pink absorption in diamond will need to take into account the findings reported here to refine our knowledge of the defect's formation.

Acknowledgements

De Beers Technologies UK are thanked for providing the samples for this study. Profs. Moreton Moore and Bob Jones, as well as members of the De Beers Technologies UK staff are thanked for their discussions and input on this research, some of who also undertook sample preparation and characterization. Drs John Chapman and Eloise Gaillou are thanked for their helpful reviews and valuable comments that improved this manuscript. The authors acknowledge the facilities, and the scientific and technical assistance, of the Australian Microscopy and Microanalysis Research Facility at the ACMM, Sydney University, especially that of Dr Pat Trimby. SP acknowledges funding from the Australian Research Council (DP120102060, FT1101100070). Some of the analytical data were obtained using instrumentation funded by the DEST Systemic Infrastructure Grants, ARC LIEF, NCRIS, industry partners and Macquarie University. This is contribution 502 from the ARC Centre of Excellence for Core to Crust Fluid Systems (www.ccfs.mq.edu.au) and 957 from the GEMOC Key Centre (www.gemoc.mq.edu.au).

References

Buerger, M.J. (1945) The genesis of twin crystals. Journal of the Mineralogical Society of America, 30, 469-482.

Byrne, K.S., Anstie, J.D., Chapman, J., and Luiten, A.N. (2012) Infrared microspectroscopy of natural Argyle pink diamond. Diamond and Related Materials, 23, 125-129.

Cao, Y., Wang, Y.B., Chen, Z.B., Liao, X.Z., Kawasaki, M., Ringer, S.P., Langdon, T.G., and Zhu, Y.T. (2013) De-twinning via secondary twinning in face-centered cubic alloys. Materials Science & Engineering A, 578, 110–114.

Christian, J.W., and Mahajan, S. (1995) Deformation twinning. Progress in Materials Science, 39, 1-157.

Collins, A.T. (1980) Vacancy enhanced aggregation of nitrogen in diamond. Journal of Physics C: Solid State Physics, 13, 2641-2650.

Collins, A.T. (1982) Colour centres in diamond. Journal of Gemmology, 18, 37-75.

Collins, A.T., Kanda, H., and Kitawaki, H. (2000) Colour changes produced in natural brown diamonds by high-pressure, high-temperature treatment. Diamond and Related Materials, 9, 113-122.

De Vries, R.C. (1975) Plastic deformation and “work-hardening” of diamond. Materials Research Bulletin, 10, 1193-1200.

Fisher, D. (2009) Brown diamonds and high pressure high temperature treatment. Lithos, 112, 619-624.

Fisher, D., Sibley, S.J., and Kelly, C.J. (2009) Brown colour in natural diamond and interaction

between the brown related and other colour-inducing defects. Journal of Physics: Condensed Matter, 21, 364213.

Gaillou, E., Post, J.E., Bassim, N.D., Zaitsev, A.M., Rose, T., Fries, M.D., Stroud, R.M., Steele, A., and Butler, J.E. (2010) Spectroscopic and microscopic characterization of color lamellae in natural pink diamonds. Diamond and Related Materials, 19, 1207-1220.

Gaillou, E., Post, J.E., Rose, T., and Butler, J.E. (2012) Cathodoluminescence of natural, plastically deformed pink diamonds. Microscopy and Microanalysis, 18(6), 1292-302.

Gainutdinov, R.V., Shiryaev, A.A., Boyko, V.S., and Fedortchouk, Y. (2013) Extended defects in natural diamonds: An Atomic Force Microscopy investigation. Diamond and Related Materials 40, 17-23.

Hirth, J.P., Lothe, J. (1982) The theory of dislocations. John Wiley & Sons, USA.

Hounsome, L.S., Jones, R., Martineau, P.M., Fisher, D., Shaw, M.J., Briddon, P.R., and Oberg, S. (2006) Origin of brown colouration in diamond. Physical Review B, 73, 125203.

Howell, D., Piazolo, S., Dobson, D.P., Wood, I.G., Jones, A.P., Walte, N., Frost, D.J., Fisher, D., and Griffin, W.L. (2012a) Quantitative characterization of plastic deformation of single diamond crystals: A High Pressure High Temperature (HPHT) experimental deformation study combined with Electron Backscatter Diffraction (EBSD). Diamond and Related Materials, 30, 20-30.

Howell, D., O'Neill, C.J., Grant, K.J., Griffin, W.L., Pearson, N.J., and O'Reilly, S.Y. (2012b) μ-FTIR mapping: Distribution of impurities in different types of diamond growth. Diamond and Related Materials, 29, 29-36.

Howell, D., O'Neill, C.J., Grant, K.J., Griffin, W.L., O'Reilly, S.Y., Pearson, N.J., Stern, R.A., Stachel, T. (2012c) Platelet development in cuboid diamonds: insights from micro-FTIR mapping. Contributions to Mineralogy and Petrology, 164, 1011-1025.

Kaga, H., and Gilman, J.J. (1969) Twinning and detwinning in calcite. Journal of Applied Physics, 40, 3196-3207.

Kaminsky, F.V., Zakharchenko, O.D., Griffin, W.L., Channer, D.M.De.R., and Khachatryan-Blinova, G.K. (2000) Diamond from the Guaniamo Area, Venezuela. Canadian Mineralogist, 38, 1347-1370.

Li, B.Q., Li, B., Wang, Y.B., Sui, M.L., and Ma, E. (2011) Twinning mechanism via synchronized activation of partial dislocations in face-centered-cubic materials. Scripta Materialia, 64, 852-855.

Machado, W.G., Moore, M., and Yacoot, A. (1998) Twinning in natural diamond. II. Interpenetrant cubes. Journal of Applied Crystallography, 31, 777-782.

Mineeva, R.M., Speransky, A.V., Titkov, S.V., and Zudin, N.G. (2007) The ordered creation of paramagnetic defects at plastic deformation of natural diamonds. Physics and Chemistry of Minerals, 34, 53-58.

Mineeva, R.M., Titkov, S.V., and Speransky, A.V. (2009) Structural defects in natural plastically deformed diamonds: evidence from EPR spectroscopy. Geology of Ore Deposits, 51(3), 233-242.

Ni, S., Wang, Y.B., Liao, X.Z., Li, H.Q., Figueiredo, R.B., Ringer, S.P., Langdon, T.G., and Zhu, Y.T. (2011) Effect of grain size on the competition between twinning and detwinning in nanocrystalline metals. Physical Review B, 84, 235401.

Niewczas, M. (2007) Dislocations and Twinning in Face Centred Cubic Crystals, *in* Dislocations in Solids, Eds. F.R.N. Nabarro, J.P. Hirth, p 265.

Persson, A. (1983). A first-principle calculation of the intrinsic stacking-fault energy in diamond. Philosophical Magazine A, 47(6), 835-839.

Pirouz, P., Cockayne, D.J.H., Sumida, N., Hirsch, P., and Lang, A.R. (1983). Dissociation of dislocations in diamond. Proceedings of the Royal Society London A, 386, 241-249.

Phaal, C. (1964) Plastic deformation of diamond. Philosophical Magazine, 10, 887-891.

Prior, D.J., Trimby, P.W., Weber, U.D., and Dingley, D.J. (1996) Orientation contrast imaging of microstructures in rocks using forescatter detectors in the scanning electron microscope. Mineralogical Magazine 60, 859-869.

Prior, D.J., Boyle, A.P., Brenker, F., Cheadle, M.C., Day, A., Lopez, G., Peruzzo, L., Potts, G.J., Reddy, S., Spiess, R., Timms, N.E., Trimby, P., Wheeler, J., and Zetterström, L. (1999) The application of electron backscatter diffraction and orientation contrast imaging in the SEM to textural problems in rocks. American Mineralogist, 84, 1741–1759.

Shiryaev, A.A., Frost, D.J., and Langenhorst, F. (2007) Impurity diffusion and microstructure in diamonds deformed at high pressures and temperatures. Diamond and Related Materials, 16, 503-511.

Smith, E.M., Helmstaedt, H.H., and Flemming, R.L. (2010) Survival of brown colour in diamond during storage in the subcontinental lithospheric mantle. The Canadian Mineralogist, 48, 571-582.

Taylor, W.R., Jaques, A.L., and Ridd, M. (1990) Nitrogen-defect aggregation characteristics of some Australasian diamonds: Time-temperature constraints on the source regions of pip and alluvial diamonds. American Mineralogist, 75, 1290-1310.

Titkov, S.V., Shigley, J.E., Breeding, C.M., Mineeva, R.M., Zudin, N.G., and Sergeev, A.M. (2008) Natural-color purple diamonds from Siberia. Gems & Gemology, 44, 56-64.

Titkov, S.V., Krivovichev, S.V., and Organova, N.I. (2012) Plastic deformation of natural diamonds by twinning: evidence from X-ray diffraction studies. Mineralogical Magazine, 76, 143-149.

Tomlinson, E.L., Howell, D., Jones, A.P., and Frost, D.J. (2011) Characteristics of HPHT diamond grown at sub-lithosphere conditions (10-20 GPa). Diamond and Related Materials, 20, 11-17.

Varma, C.K.R. (1970) Some observations on the reported evidence of slip during growth of natural diamond crystals. Acta Metallurgica, 18, 1113-1119.

Woods, G.S. (1986) Platelets and the infrared absorption of Type Ia diamonds. Proceedings of the Royal Society of London A, 407, 219-238.

Yacoot, A., Moore, M., and Machado, W.G. (1998) Twinning in natural diamond. I. Contact twins. Journal of Applied Crystallography, 31, 767-776.

Figure Captions

719 Figure 1: Illustration of a single (011) plane of the diamond crystal lattice. The carbon
720 atoms do not all lie exactly in a 2D plane; those slightly further back are shaded light
721 grey, and those further forward are white. The body of the crystal is shown at the
722 sides, while the twinned region is in the middle in between the two twin planes
723 (dashed red lines). Above the lattice are illustrations of 3D cubes; the three coloured
724 arrows define the three <100> directions, which also provide a visual representation
725 of the crystal orientation of the bulk and twinned regions.
726
727 Figure 2: Photos (left) and CL images (right) of each of the nine samples used in this
728 study. Inset are cube illustrations showing the orientations of the three <100> axes.
729 Scale bars represent 0.5 mm. The red boxes on each of the CL images mark the areas
730 used for EBSD mapping to gain overviews of each sample, some of which are shown
731 in **Figure 4**, while all the EBSD data are provided in **Table 3**. For the bottom three
732 pink samples, close up CL images are shown to highlight the {111} lamellae cross
733 cutting the existing growth stratigraphy. Scale bars in these three CL images are 0.1
734 mm. The arrow in the CL image of NL000-PK46-A shows a single lamella that lies
735 on a different {111} plane to all the others in that sample.
736
737 Figure 3: Impurity characteristics as determined by FTIR spectroscopy. (a) Nitrogen
738 concentration *vs* nitrogen aggregation plots for the samples analysed by EBSD in this
739 study (Tables 2 and 3). Isotherms show a range of ages (3 Ga for the thickest line to
740 100 Ma for the thinnest line) for two different temperatures; 1200^{o}C (black lines) and
741 1100^{o}C (grey lines). (b) A "regularity" plot (after Woods, 1986) of absorbance by B
742 centres *vs* platelet intensity [I(B´)] for the nine samples analysed in this study. (c) A
743 previously unpublished laboratory dataset from De Beers Technologies for pink
744 diamonds from several worldwide localities (see supplementary data). The 6 pink
745 samples from this study are also plotted to show how they fall in to the two groupings.
746
747 Figure 4: Cathodoluminescence (CL) images (left) and overview EBSD maps (right)
748 of example samples from each of the three categories of samples studied; A6-05
749 (brown), A62-06 (pink group 1) and NL000-PK11 (pink group 2). The colour scale
750 bar in the map of A62-06 shows the degree of misorientation relative to a specific
751 point (chosen as that the data point in the bottom left corner). Its scale is applicable to
752 all three EBSD maps. Deformation lamellae are visible in the CL images of all three

753 samples but they do not appear in the EBSD maps, nor show any relationship to the
754 deformation depicted in the overview maps. Scale bars represent 0.25 mm.
755
756 Figure 5: A selection of images highlighting the effectiveness of orientation contrast
757 (OC) imaging to pick out {111} deformation lamellae as microtwins, at a range of
758 scales. Images (a) and (b) are secondary electron (SE) and OC images of NL000-
759 PK01. Note how the microtwins are seen only in the OC image, while the SE image
760 shows a completely flat surface. The remaining images are of (c) NL000-PK11 and
761 (d-f) NL000-PK46-A. Note how in images (b) and (c) not all the twins extend across
762 the full width of the crystal; those that terminate within the crystals are picked out by
763 arrows in each image. Image (f) shows how when two microtwins, each one on a
764 different {111} plane, cross each other, there appears to be a small cavity at the point
765 of intersection.
766
767 Figure 6: Orientation contrast (OC) images showing where high-resolution EBSD
768 maps collected on pink diamonds NL000-PK11, NL000-PK46-A and NL000-PK01
769 revealed the presence of microtwins. The orientations of the bulk crystal and
770 microtwins are shown by the inset cube illustrations.
771
772 Table 1: The main characteristics and primary spectroscopic defects observed in
773 group 1 and group 2 pink diamonds as defined by Gaillou et al. (2010; 2012;
774 references therein). “x” indicates the presence and “o” the absence of the defined
775 colour centre, while “(+)” indicates the dominant centre and “(-)” the one that is less
776 intense (after Gaillou et al., 2010).
777
778 Table 2: The primary characteristics, including source location and FTIR data, of the
779 9 samples analysed in this study. Uncertainties in the nitrogen concentration and
780 aggregation data are ±10%. The platelet areas are accurate to ±20 cm^{-2}, and their
781 position to 1 cm^{-1}.
782
783 Table 3: Summary of the EBSD mapping data obtained for all 9 samples.
784
785 Supplementary data: FTIR data for the large number of pink samples from various
786 localities worldwide, plotted in Figure 3b.

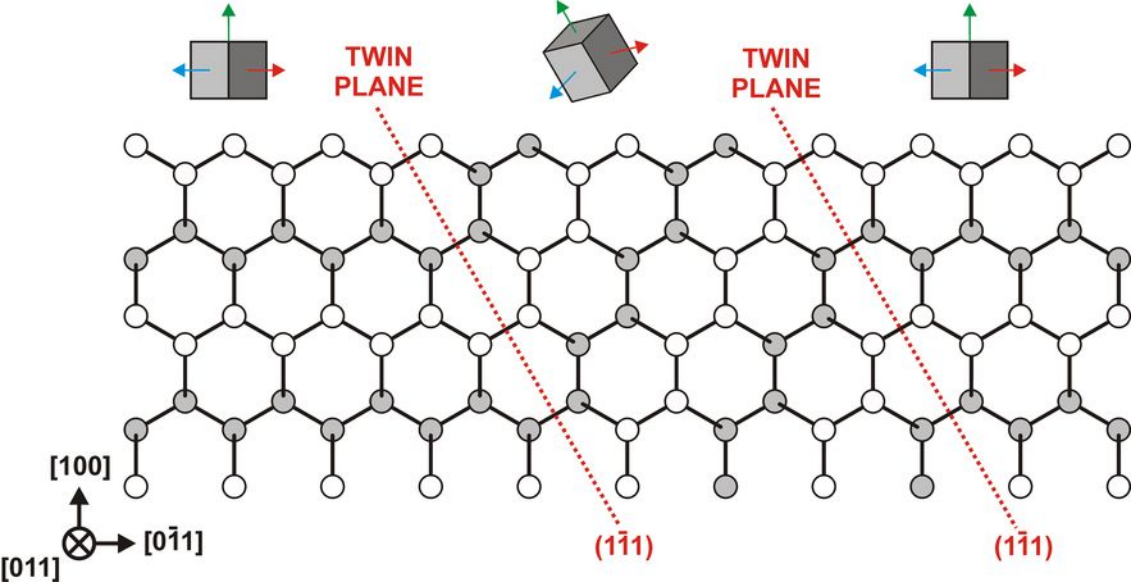
TWIN
PLANE
TWIN
PLANE
[100]
[011]
[0$\bar{1}$1]
(1$\bar{1}$1)
(1$\bar{1}$1)

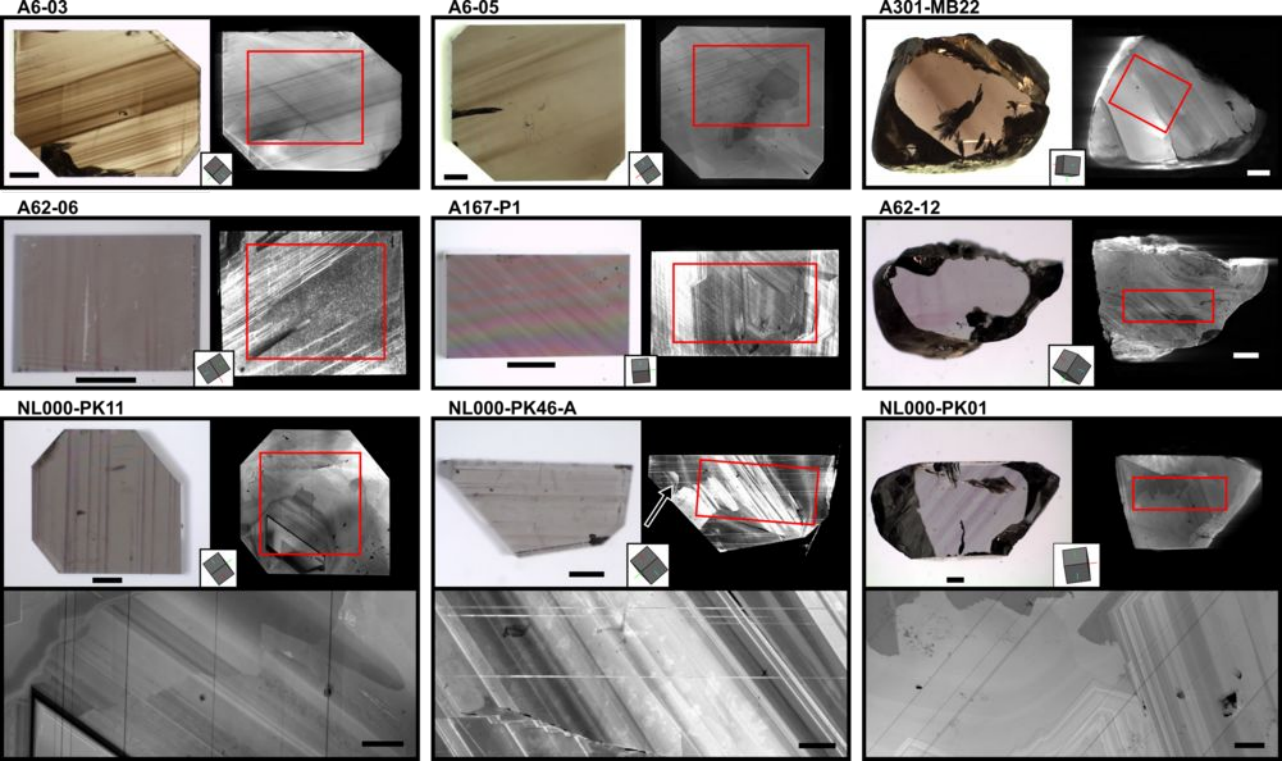
A6-03
A6-05
A301-MB22
A62-06
A167-P1
A62-12
NL000-PK11
NL000-PK46-A
NL000-PK01

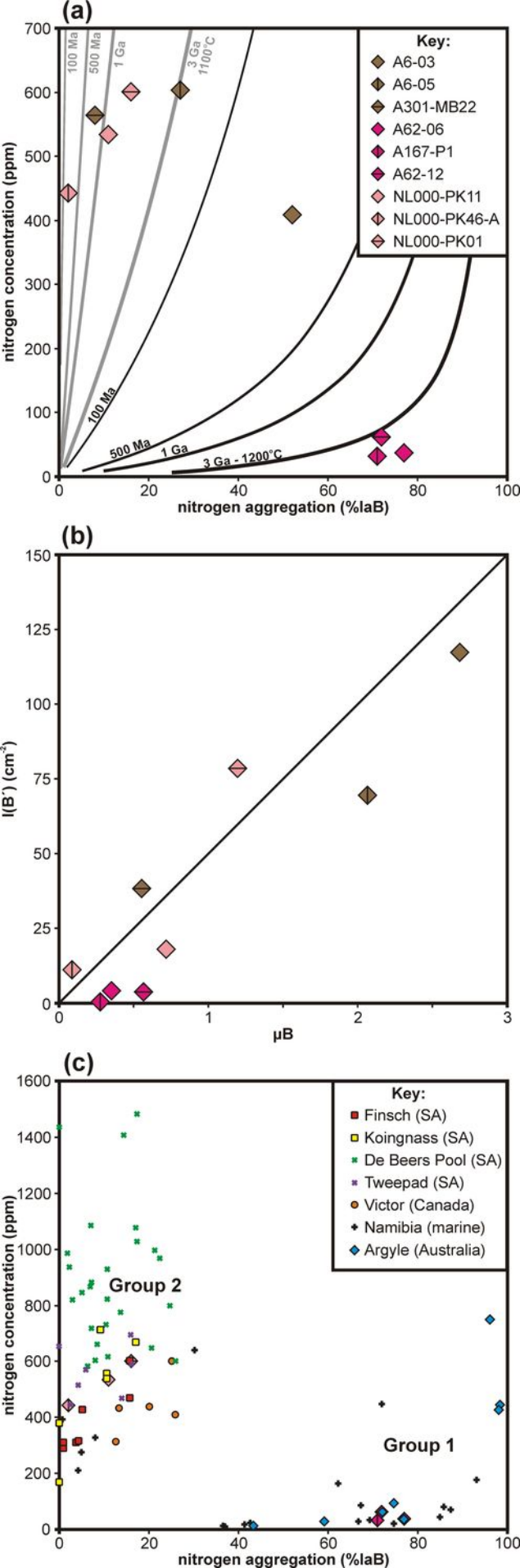
(a)
nitrogen concentration (ppm)
nitrogen aggregation (%IaB)
100 Ma
500 Ma
1 Ga
3 Ga
1100°C
100 Ma
500 Ma
1 Ga
3 Ga - 1200°C
Key:
A6-03
A6-05
A301-MB22
A62-06
A167-P1
A62-12
NL000-PK11
NL000-PK46-A
NL000-PK01
(b)
I(B') (cm⁻²)
μB
(c)
nitrogen concentration (ppm)
nitrogen aggregation (%IaB)
Group 2
Group 1
Key:
Finsch (SA)
Koingnass (SA)
De Beers Pool (SA)
Tweepad (SA)
Victor (Canada)
Namibia (marine)
Argyle (Australia)

(a) A6-05 - Brown

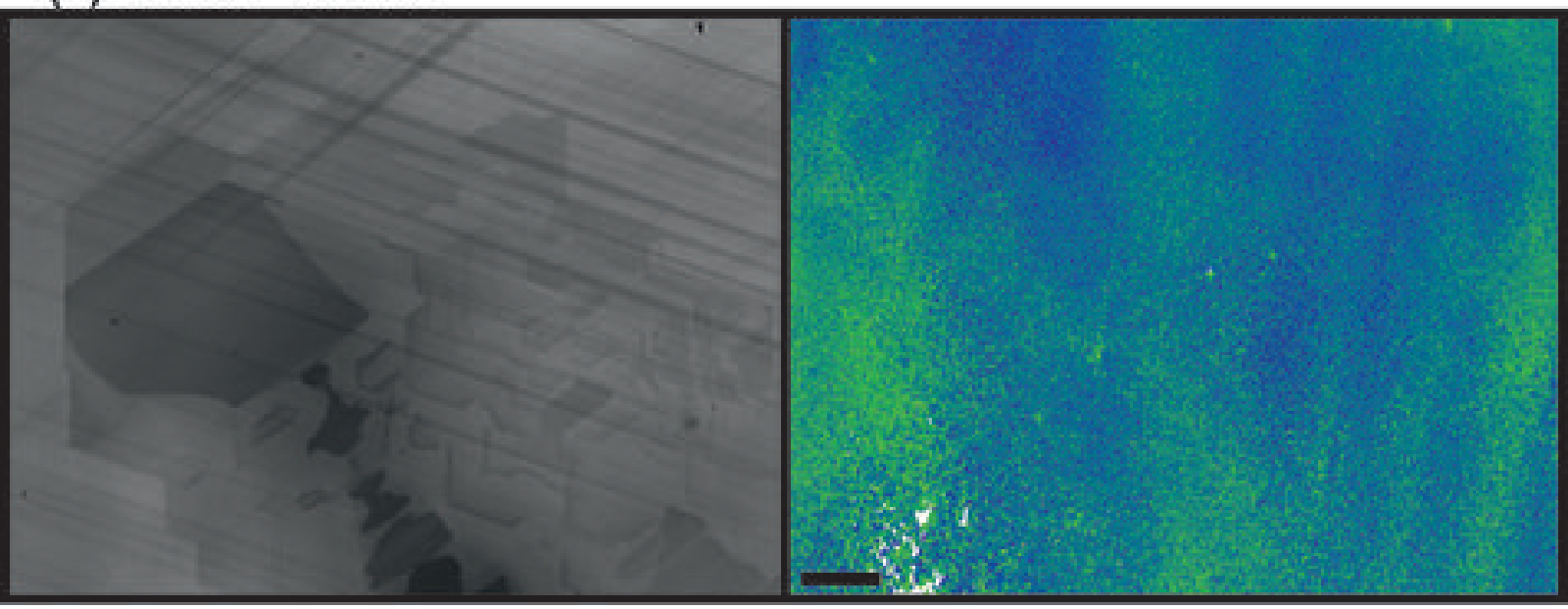

(b) A62-06 - Pink group 1

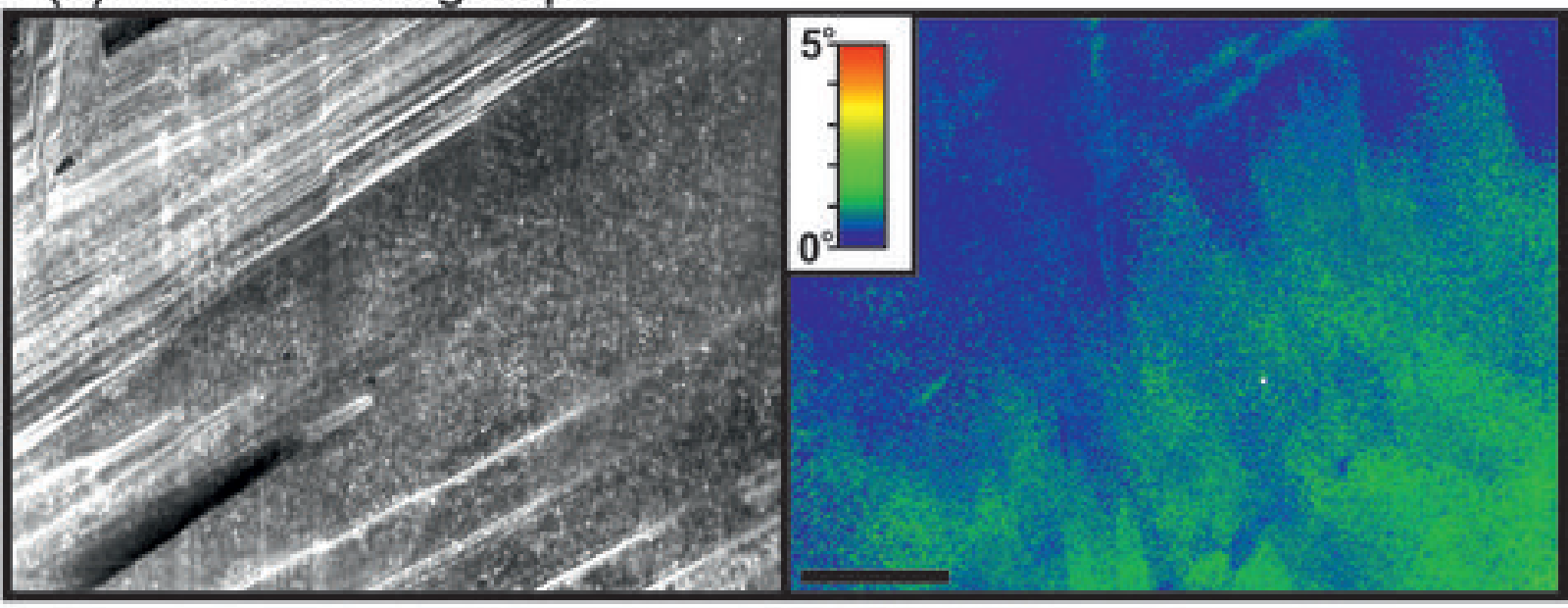

(c) NL000-PK11 - Pink group 2

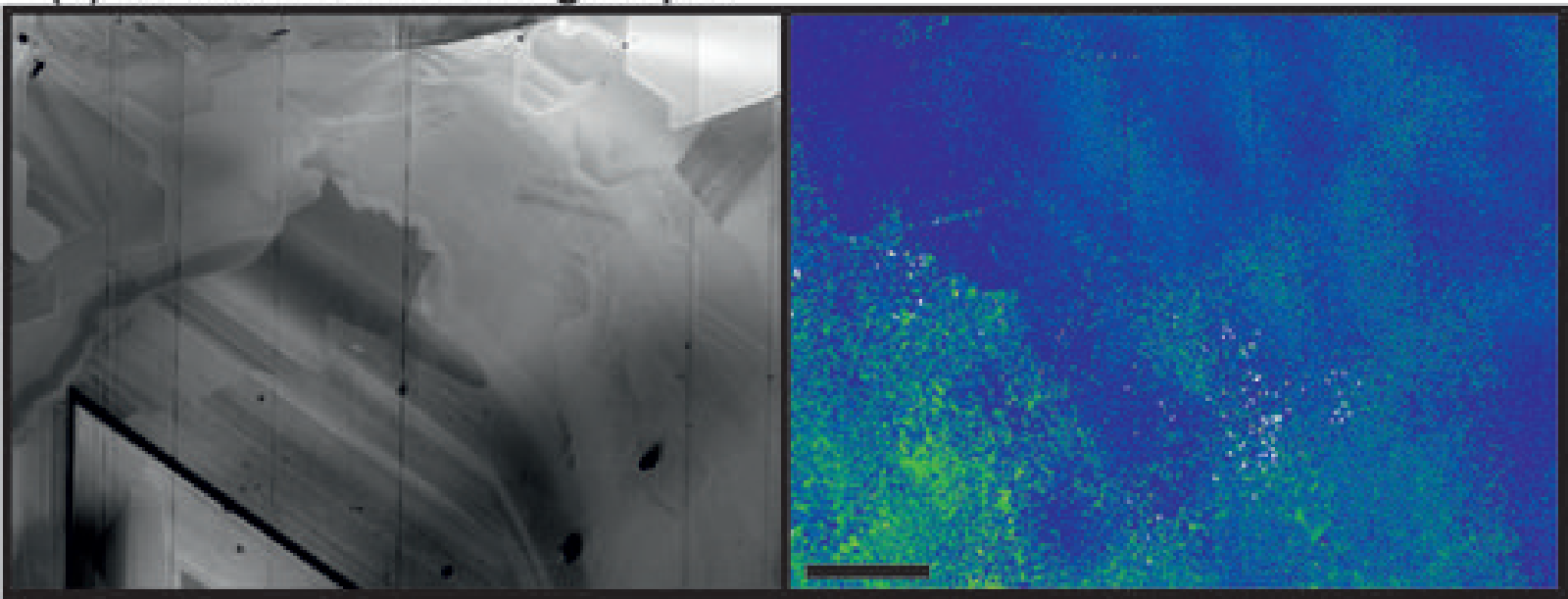

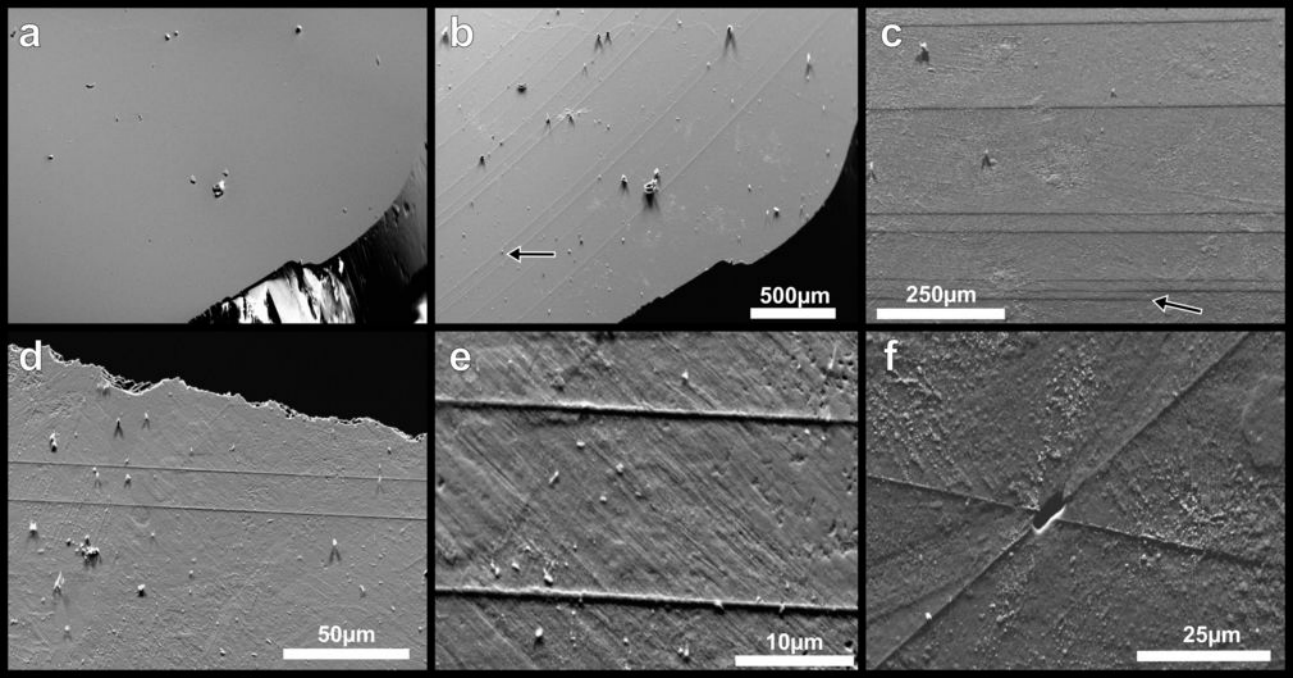
a
b
500μm
c
250μm
d
50μm
e
10μm
f
25μm

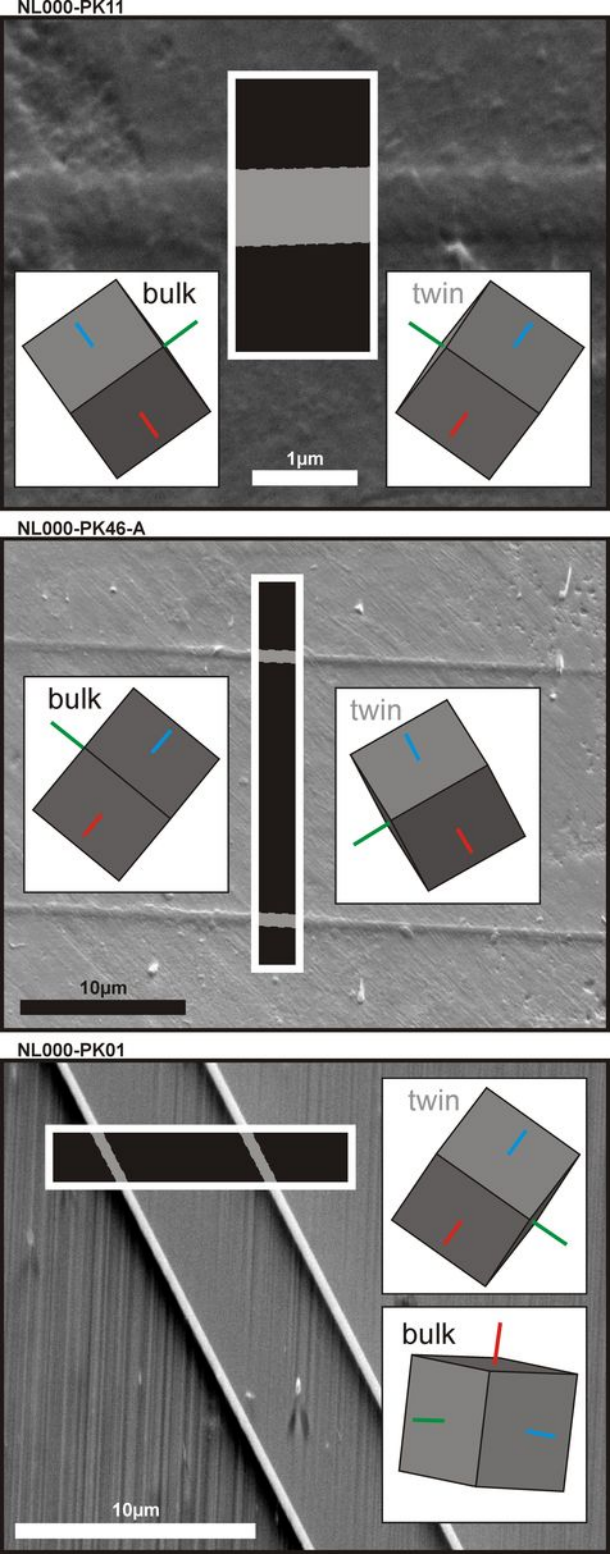
NL000-PK11
bulk
twin
1µm
NL000-PK46-A
bulk
twin
10µm
NL000-PK01
twin
bulk
10µm

	Group 1	Group 2
Origin	Argyle, St Elena	Everywhere else
Colour absorption	550-560nm	550-560nm
Colour distribution	Not only restricted to the lamellae	Restricted to lamellae
lamellae appearance	Wavy	Straight
lamellae = twins	?	Yes
N cctn	< 300 ppm	> 400ppm
Agg	> 50% IaB	< 50% IaB

Defect	bulk crystal	lamellae	bulk crystal	lamellae
390 nm	x	o	x	o
405.5 (N3-X)	o	o	o	x
415.5 (N3)	x(+)	x(-)	o	o
425 (Blue Band)	o	o	x	o
503.2 (H3)	x(-)	x(+)	o	x

						Platelets			
Sample #	Colour	Source	FTIR Type	N ppm	%IaB	area (cm^{-2})	position (cm^{-1})	H @ 3107	Group
A6-03	brown	unknown	IaA**B**	409	52	117.3	1361	Y	Brown
A6-05	brown	unknown	Ia**A**B	603	27	69.5	1365	Y	Brown
A301-MB22	brown	unknown	Ia**A**B	564	8	38.3	1366	Y	Brown [1]
A62-06	pink	Argyle	IaA**B**	36	77	4.1	1376	Y	Group 1 pink
A167-P1	pink	unknown	IaA**B**	31	71	0.4	1361	Y	Group 1 pink
A62-12	pink	Argyle	IaA**B**	62	72	3.7	1361	Y	Group 1 pink
NL000-PK11	pink	Koingnass, SA	Ia**A**B	534	11	18.0	1372	Y	Group 2 pink
NL000-PK46-A	pink	Tweepad, SA	near IaA	443	2	11.1	1371	Y	Group 2 pink
NL000-PK01	pink	Finsch, SA	Ia**A**B	601	16	78.5	1366	Y	Group 2 pink

[1] Also shows "amber centre" at 4163 cm^{-1}

Table 3: Summary of the EBSD mapping data obtained for all 9 samples

Sample #	Map area (um^2)	Step size (um)	Mean misorientation (^{o})
Brown			
A6-03	3001392	4	0.75
A6-05	3427398	3	0.86
A301-MB22	1000100	5	0.96
Group 1 pink			
A62-06	1343424	4	0.49
A167-P1	1265744	4	1.11
A62-12	640000	8	0.79
Group 2 pink			
NL000-PK11	1771808	4	0.46
NL000-PK46-A	1273600	10	0.94
NL000-PK01	767700	10	0.57